Shear-dominated Interlaminar Fracture Process in CFRP Composite Laminates

Seyed Saeid Rahimian Koloor, Norizah Redzuan, Mohd Nasir Tamin*

Faculty of Mechanical Engineering, Universiti Teknologi Malaysia,
81310 UTM, Skudai, Johor, MALAYSIA

Abstract: This paper examines and quantifies the mechanics of damage processes leading to interlaminar fracture of composite laminates under shear-dominated loading. For this purpose a 16-ply unidirectional CFRP composite laminate specimen with end-notched flexural (ENF) geometry is tested in a 3-point bend test set-up. The initial crack length to span ratio is a/L = 0.325. The long span of 160 mm induces a gradual evolution of shear-dominated interlaminar damage and fracture. Finite element (FE) simulation of the test is performed with interlaminar cohesive behavior assumed for the mid-thickness pre-cracked interface. The measured load-deflection of the ENF specimen is used to validate the FE model with cohesive interface. Hypothetical elastic CFRP composite beams with and without interlaminar edge crack are also modelled as reference cases. Results show that the initial crack reduces flexural stiffness by 30.2 pct. with insignificant lamina damage. Interlaminar shear stress and the corresponding shear energy release rate govern the interlaminar fracture process in the cohesive zone. A cohesive zone length of 2.2 mm with maximum relative shear displacement of 0.023 mm is predicted at the onset of interlaminar fracture. The rate of energy dissipation due to interlaminar damage accelerates to 3.75 N.mm/sec in the final 9 pct. of the displacement load step, indicating sudden crack propagation as observed experimentally.

Keywords: CFRP Composite laminates, Cohesive interface, end-notch flexure, Finite Element simulation, interlaminar fracture.

1. Introduction

Carbon fiber reinforced polymer (CFRP) composite laminates offer attractive structural properties of high strength-to-weight ratio and high specific modulus combined with design flexibility through sequencing of the pre-impregnated laminates. These characteristics have continuously been exploited in advanced structural applications such as skin of aircraft wings, automotive body panels, stringers, molded beams and floor panels. General loading and boundary conditions of these structures often involve lateral bending of the composite laminates. Such flexural loading induces simultaneous tension-compression stresses in the lamina with varying magnitude of shear stresses acting in lamina interfaces. The inherently weak lamina interfaces renders interface delamination as the dominant mechanism in the failure process of fiber reinforced polymer (FRP) composite laminates [1-3]. However, matrix damage manifested in the form of hackles has also been observed on the damaged and fractured surfaces. Interface delamination accounted for up to 46.7 pct. reduction in flexural stiffness from undamaged state in a 12-ply CFRP composite laminates with anti-symmetric ply sequence under three-point bending [4]. In addition, such significant loss of stiffness and load-carrying capacity occur in the absence of any visible damage of the CFRP composite structure. In this respect, the continual process of damage leading to catastrophic fracture of CFRP composite laminates should be quantified and thoroughly understood as an integral part of design and reliability assessment of the composite structures.

Mechanics of FRP composite laminates could be quantified with the aid of numerical modeling by finite element (FE) method and validation testing on the respective composite samples. Reliable FE simulation outcomes rely on three major aspects. The modeling aspect requires accurate representation of the composite part geometry, prescribed loading and boundary conditions, correct description of constitutive behavior of the lamina and interfaces, and credible criteria for failure of these phases. Each lamina is often represented by an orthotropic continuum plate in the meso-scale modeling. Failure of the lamina has been described by several theories including stress-based criteria [5,6] and strain-based criteria [7]. Interface decohesion model has been formulated for simulating delamination in bi-material interfaces [8,9]. The analysis aspect demands correct physical interpretation of FE-calculated results in relation to the assumptions made. The validation aspect calls for independent solution, often through experimental measurements of deformation response of the composite structure. Performance of these failure criteria and damage-based models for FRP composite laminates can be found in open literature [10-13]. However, limited studies are available on quantitative description of deformation and failure process in CFRP composite laminates.

*Corresponding author: E-mail: taminmn@fkm.utm.my; Tel: +60-12-778-1410; Fax: +60-7-556-6159

This paper investigates deformation response and failure process in CFRP composite laminates under flexure loading. It gives a quantitative description of the mechanics and damage process leading to the catastrophic interlaminar fracture.

2. CFRP composite and experimental procedures

A 16-ply unidirectional CFRP composite laminate, $[0]_{16}$ with pre-existing interface crack is used as a demonstrator material in this study. Each lamina consists of unidirectional high modulus carbon fibers and epoxy resin (M40J fibers and NCHM 6376 resin, Structil, France). The CFRP composite sample measured 190 x 25 mm^2 with thickness of 2.46 mm. The 0^o fiber orientation coincides with the longitudinal direction of the specimen. A 14 μm-thick Teflon film insert was positioned in the mid-thickness interface along one edge of the laminate during fabrication to create an artificial pre-cracked interface with a straight crack front in the specimen.

The resulting end-notched flexural (ENF) specimen is loaded in a 3-point bend test set-up as illustrated in Fig. 1. The initial crack length and span is 52 and 160 mm, respectively (a/L = 0.325). The loading and support rollers are of 10 mm-diameter. The relatively long span is intended to facilitate delamination failure in the interface ahead of the initial interface crack front. Loading is provided by controlled displacement of the central loading roller to a prescribed 16.5 mm-deflection at a rate of 3 mm/min. Load-central deflection data pairs are recorded at regular time intervals throughout the test.

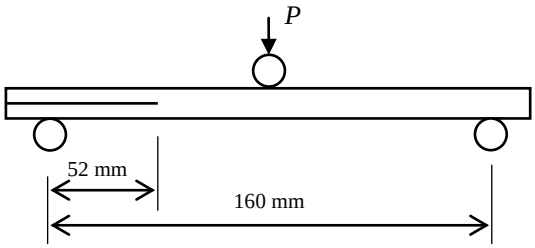

Fig. 1 Test set-up of 3-point bending with ENF composite laminate specimen.

Figure 2 shows the measured load-deflection response of the ENF composite specimen at the mid-span location. A reference dashed straight line is superimposed on the plot. An initial linear load-deflection line up to 10.5 mm indicates elastic response of the material. The corresponding effective bending stiffness of the pre-cracked CFRP composite as depicted by the slope of the curve is 25.49 N/mm. In an earlier study of flexural response of similar CFRP composite sample, but without initial crack a load-deflection curve featuring a continuously decreasing stiffness since early loading was observed. Such degrading flexural stiffness is attributed primarily to damage of the lamina [14]. Thus, it is postulated in this study that lamina damage is insignificant and failure of the ENF specimen is governed by delamination from the pre-existing interface crack front. Continuous strength degradation of the critical mid-section interface is manifested in the decreasing slope of the curve. This postulate is examined and its validity established in subsequent FE simulation of the experiment. While slight load drop following the attainment of the peak level reflects inherent limited toughness of the interface, the sudden fracture at the final deflection of 16.5 mm indicates catastrophic delamination event.

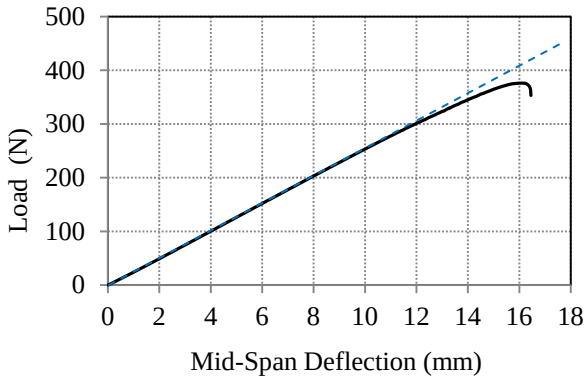

Fig. 2 Measured load-deflection response at mid-span location of the ENF specimen.

3. Finite element modeling

Damage and failure process of the CFRP composite specimen with pre-existing interface crack is simulated using continuum damage mechanics-based approach. In this approach, each composite lamina is represented by an equivalent homogeneous orthotropic material. The geometry, mesh and boundary conditions of the FE model used are illustrated in Fig. 3. Dimensions of the ENF specimen model are identical to the experimental counterpart (see Fig. 1). The model is partitioned into 16 layers in the thickness direction, each representing a unidirectional lamina. The lamina model was meshed using 8-node linear continuum elements (C3D8R) with reduced integration [15]. Such reduced-integration elements are capable of controlling hour-glass and eliminating shear locking effects in flexure-dominated loading cases. A layer of cohesive interface elements (COH3D8) are prescribed in the mid-thickness interface to capture the measured interlaminar failure. These *zero-thickness* interface elements have element mesh with matching nodes to those of solid elements on mating surfaces. An initial traction-free interface crack was simulated by releasing nodal constraints of cohesive elements residing in the crack face region. Influence of mesh density on the predicted flexural response of CFRP composite laminate specimens has been examined in previous studies [3]. Element mesh is optimized with higher mesh density in the vicinity of the crack tip and loading roller contact regions, in view of the expected localized stress gradients. The resulting number of continuum and cohesive elements used is 44160 and 1840, respectively.

Loading and support rollers are assumed to behave as analytically rigid bodies with frictionless contact onto the specimen. The support rollers are constrained from linear displacement in the three coordinate directions while the loading roller applies the prescribed vertical displacement. In addition, an arbitrary material point (node) in the middle section of the model is constrained to avoid rigid-body motion.

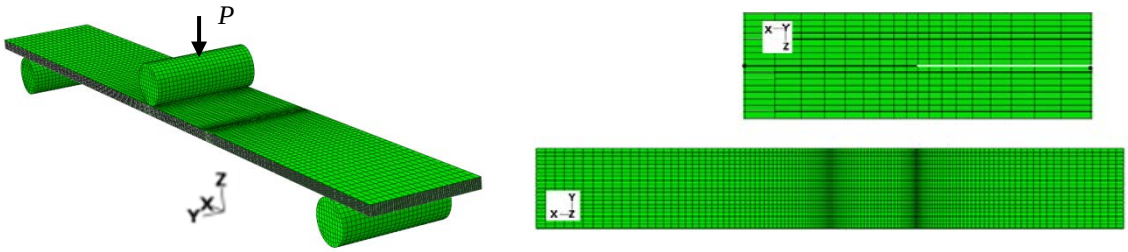

(a) (b)

Fig. 3 (a) FE model of CFRP composite specimen under 3-point bend test setup. (b) Element mesh density for each lamina (bottom) and in the interface crack tip region (top).

Three different FE simulation cases are performed as detailed in Table 1. The lamina is assumed to behave elastically without experiencing any damage. Properties and relevant materials data for the unidirectional CFRP composite lamina and interface are listed in Table 2 [3,13,16-18]. Material coordinate direction-11 is oriented along the 0^o fiber direction.

Table 1. FE simulation cases

Case ID	Description
A1	Perfect interface bonding but without initial crack
A2	Perfect interface bonding and with initial crack
B1	Cohesive interface with initial crack

3.1 *Cohesive Zone Model*

Delamination failure process of a material point on the interface is described using cohesive zone model, as detailed elsewhere [13]. The failure process begins with damage initiation followed by damage propagation to separation of the adjacent material points. The thin interface is acted upon only by shear and normal tractions. It is assumed, as a first approximation that the interface behavior is adequately described by a bilinear traction-relative displacement softening law as illustrated in Fig. 4. In pure delamination mode (opening Mode I, shearing Mode II or III) the onset of damage occurs when the tensile normal $\langle\sigma_{33}\rangle$ or shear traction (τ_{31}, τ_{32}) attained their respective tensile *(T)* or shear strength *(S)* of the interface, respectively.

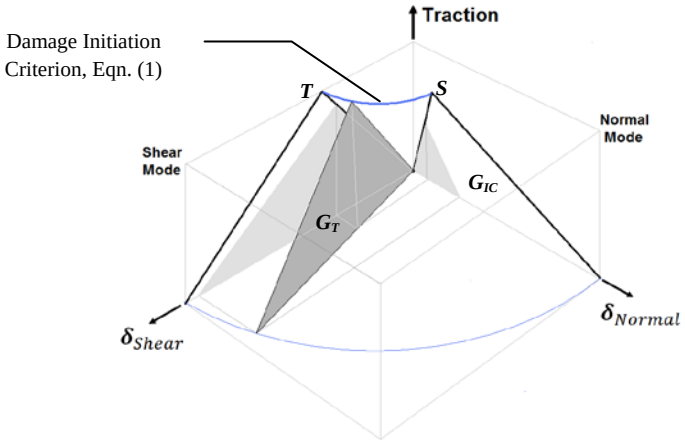

Fig. 4 Illustration of traction-displacement softening law for interface under mixed mode loading

Table 2. Elastic properties of unidirectional CFRP composite lamina and interface.

Lamina propertties		
Elastic modulus	E_{11}	103 GPa
	E_{22}	7 GPa
	E_{33}	7 GPa
Shear modulus	G_{12}	3.15 GPa
	G_{13}	3.15 GPa
	G_{23}	2.75 GPa
Poisson's ratio	ν_{12}	0.34
	ν_{13}	0.34
	ν_{23}	0.3
Interface properties		
Elastic modulus	E	0.974×10^6 MPa
Shear modulus	$G_1 = G_2$	0.34×10^6 MPa

A stress-based damage initiation criterion is given by eqn. (1) [13, 19] and illustrated in Fig. 4 as:

$$\sqrt{\left(\frac{\langle\sigma_{33}\rangle}{T}\right)^2+\left(\frac{\tau_{31}}{S}\right)^2+\left(\frac{\tau_{32}}{S}\right)^2}=1 \tag{1}$$

For a small cohesive zone, the critical energy released rate in the respective fracture mode can be estimated by the area under the traction-displacement curve for Mode I and Mode II, respectively as illustrated in Fig. 4. Damage propagation under mixed-mode loading is predicted in terms of the total energy release rates, $G_T = G_I+G_{II}$ and single-mode fracture toughness, G_{IC} and G_{IIC} as [20]:

$$G_T = G_{IC} + \left(G_{IIC} - G_{IC}\right)\left(\frac{G_{II}}{G_T}\right)^{\eta} \tag{2}$$

The parameter, η describes the interaction of fracture modes with typical value, determined experimentally for laminated composite samples as listed in Table 3 [21] along with other parameter values for the cohesive zone model.

Table 3. CZM parameter values for CFRP composite interface

Damage-related properties		
Tensile strength	T	58.2 MPa
Shear strength	S	69.6 MPa
Critical energy release rate (Mode I)	G_{IC}	0.5 N/mm
Critical energy release rate (Mode II and III)	$G_{IIC} = G_{IIIC}$	1.73 N/mm
Mode mixity	η	1.45

4. Results and discussion

Results of FE simulation are presented and discussed in terms of load-deflection response, characteristic evolution of interface stresses and damage variable, and damage dissipation energy.

4.1 *Load-deflection response*

The predicted load-deflection curves of the CFRP composite sample for the different cases are compared with measured curve as shown in Fig. 5. Flexural stiffness of a crack-free specimen (Case *A1*) is 36.52 N/mm while that with a pre-existing crack of length 52 mm (Case *A2*) is 25.49 N/mm. Simulation of pre-cracked specimen with damaging interface (Case *B1*) also predicted identical flexural stiffness prior to damage initiation. Thus, the existence of the 52 mm-crack reduces flexural stiffness of the CFRP composite laminate specimen by 30.2 pct. This loss of stiffness also indicates reduction in lateral load-carrying capability of the laminate with pre-existing defect. Identical slope of the curves for Case *A2* and Case *B1* with that measured experimentally, up to deflection of 10.5 mm suggests that the occurrence of lamina damage is insignificant in the current test configuration for the unidirectional CFRP composite laminate. Additional deflection induces delamination damage as manifested in the gradual decrease of the flexural stiffness. FE model without consideration of interface damage (Case *A2*) is incapable of capturing degradation behavior or failure process of the interface. A drastic change in the slope of the curve suggests the occurrence of interface crack propagation, as will be discussed in the next section. The predicted maximum load level of 372 N achieved at the end of the test compared well with measured value. However, the observed unstable interlaminar crack propagation could not be accounted for with the current damage model.

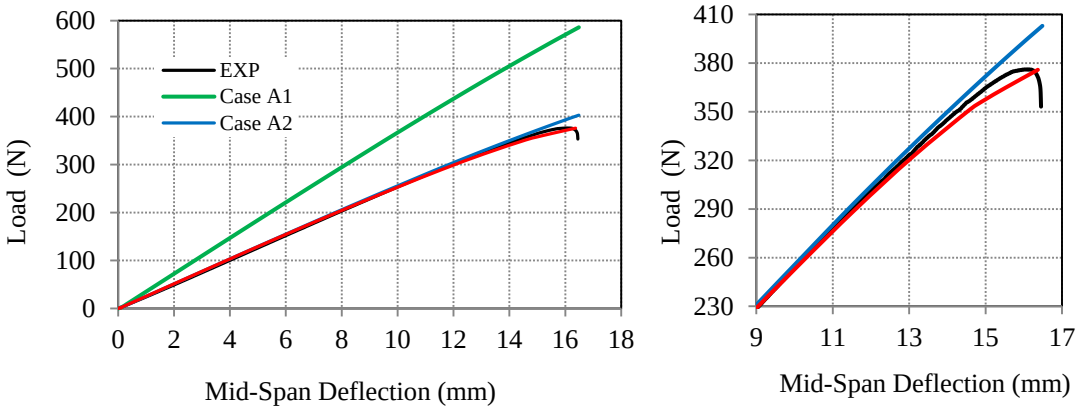

Fig. 5. Comparison of predicted load-deflection responses with measured curve for the CFRP composite laminate sample under 3-point bending. Inset figure enlarges details of the nonlinear part.

4.2 *Characteristic evolution of interface stresses and damage variables*

Characteristic evolution of damage variables for damage initiation and propagation process at a generic material point in the cohesive interface is shown in Fig. 6a. The quadratic damage initiation characteristic is governed by eqn. (1) with the value of unity indicating that the criterion is satisfied for the onset of damage (point marked *A)*. Subsequently, another damage variable quantifying damage evolution is monitored. The nonlinear characteristic damage evolution as governed by eqn. (2) is based on energy release rates under combined loading modes. A value of unity for this variable indicates separation of the adjacent material points. The corresponding evolution of the resultant shear stress and normal stress at the same material point on the interface is shown in Fig. 6b. The test set-up induces dominant interface shear stress over the normal stress counterpart. The resultant shear stress increases linearly reaching the peak value at the onset of damage (point marked *A*). The stress then decreases nonlinearly as dictated by the continuous energy released during damage evolution phase. This condition is also reflected through the gradual decrease in flexural stiffness of the composite specimen. The stresses diminish upon separation of the material point (Point marked *B*). This characteristic evolution of interface stresses and damage is experienced by every material point in the interface undergoing interlaminar fracture process. Collection of separated material points on the interface is interpreted in this study as representing new interlaminar crack surfaces.

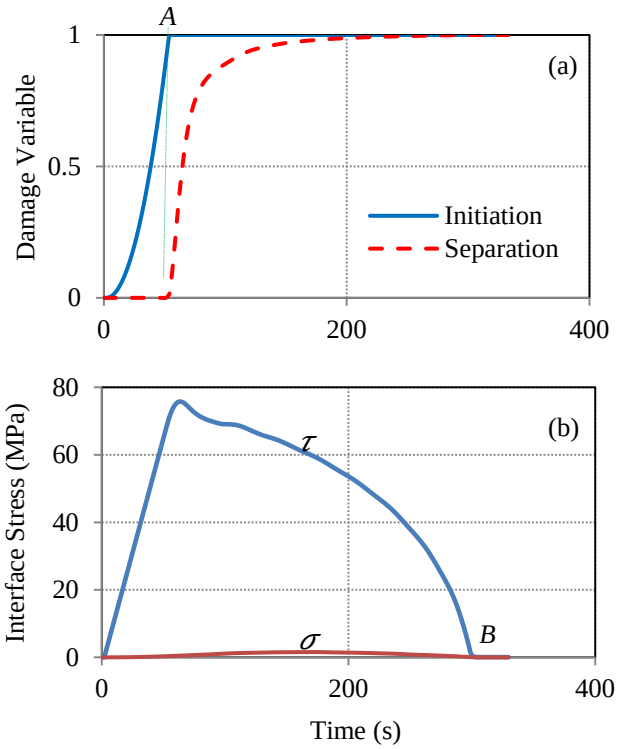

Fig. 6 Evolution of (a) damage variables and (b) stresses at a material point on the interface crack front during loading.

The nature of cohesive zone at the interface is examined in terms of shear displacement of adjacent laminar surfaces in the mid-thickness interface plane containing the crack. In view of shear-dominant interface loading, the shear displacement of these points is shown in Fig. 9 for two different loading steps corresponding to the onset of damage (deflection, d = 2.7 mm) and when separation of the critical material point commences (d = 10.5 mm). The initial crack tip is located at the point marked *C*. Results show that a cohesive zone of length 2.2 mm (given by the horizontal path *C*-*D*) with maximum relative shear displacement of 0.023 mm is formed at the onset of interlaminar fracture. Slight nonlinear variation of relative shear displacement along the cohesive zone length is acknowledged.

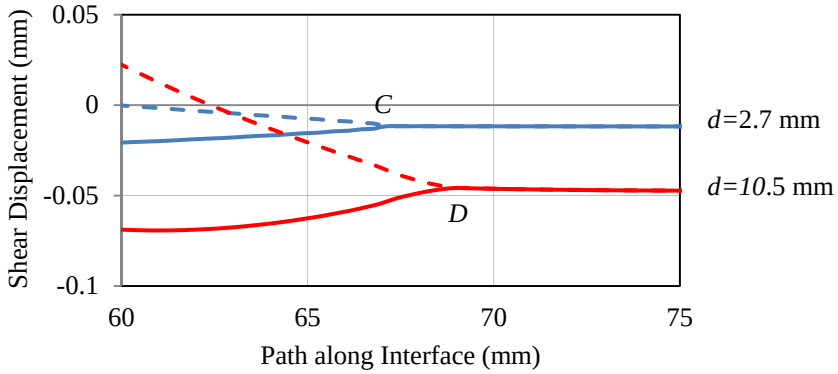

Fig. 9 Shear displacements of the interface illustrating the formation of cohesive zone ahead of the pre-existing interface crack tip.

4.3 *Damage dissipation energy*

Damage dissipation energy is the irrecoverable work expanded in the composite interface during interlaminar fracture process. It is assumed in this study that delamination process is concentrated in the mid-thickness pre-cracked interface of the ENF specimen. Exponential evolution of the interface damage dissipation energy throughout flexural loading is predicted, as shown in Fig. 10. The corresponding limited changes in flexural stiffness of the specimen are illustrated on the same plot. Although interface separation initiated very early in the specimen (onset of separation at deflection of 10.5 mm), the rate of energy dissipation by interface delamination is significant towards the end of

applied deflection (~14 mm) when sufficiently large new crack surfaces are formed. The energy dissipation due to interlaminar damage accelerates to 3.75 N.mm/sec in the final 9 pct. of the displacement load step. Such high energy dissipation rate leads to the observed unstable interlaminar crack propagation.

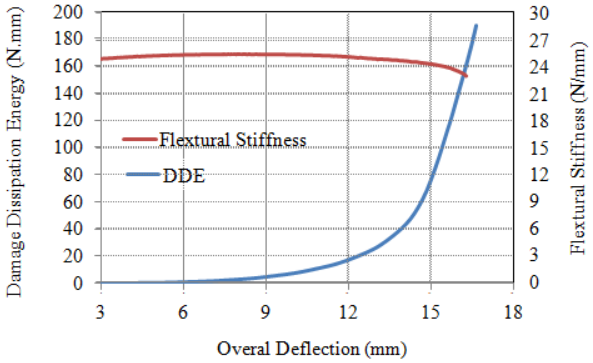

Fig. 10 Evolution of interface damage dissipation energy and flexural stiffness in the ENF specimen during the 3-point bending test.

5. Conclusions

Interlaminar fracture process in CFRP composite laminates has been quantified using a validated FE simulation of ENF specimen under 3-point bending. Results show that:

- The existence of an initial crack, $a/L = 0.325$ reduces flexural stiffness by 30.2 pct. with insignificant lamina damage.
- Interlaminar shear stress and the corresponding shear energy release rate govern the interlaminar fracture process in the cohesive zone.
- A cohesive zone length of 2.2 mm with maximum relative shear displacement of 0.023 mm is predicted at the onset of interlaminar fracture.
- The rate of energy dissipation due to interlaminar damage accelerates to 3.75 N.mm/sec in the final 9 pct. of the displacement load step, indicating sudden crack propagation.

Acknowledgment

This work is part of an on-going collaborative research program between the Institute of Automotive and Transportation (ISAT), University of Burgundy, Nevers, Cedex, France and Universiti Teknologi Malysia (UTM). Computational work is performed at High Performance Computing Center, CICT, UTM. Financial support through research grant No. RUG-00H51 is acknowledged.

References

[1] Compston P, Jar P-YB, Burchill PJ, Takahashi K. The effect of matrix toughness and loading rate on the mode-II interlaminar fracture toughness of glass-fibre/vinyl-ester composites. Composites Science and Technology 2001;61: 321-333.

[2] Arai M, Sasaki T, Hirota S, Ito H, Hu N, Quaresimin M. Mixedmodes interlaminar fracture toughness of CFRP laminates toughened with CNF interlayer. Acta Mechanica Solida Sinica 2012; 25(3): 321- 330.

[3] Koloor SSR, Hussin H, Tamin MN. Mode-I fracture characterization of CFRP laminated composites. Advanced Materials Research 2012;488-489:552-556.

[4] Koloor SSR, Abdul-Latif A, Tamin MN. Mechanics of composite delamination under flexural loading. Key Engineering Materials 2011; 462-463: 726-731.

[5] Hashin Z, Rotem A. A fatigue failure criterion for fiber reinforced materials. Composite Materials 1973; 7: 448.

[6] Tsai SW, Wu EM. A general theory of strength for anisotropic materials. Composite Materials 1971; 5: 58.

[7] Camanho, PP, Davila CG. Mixed-mode decohesion finite elements for the simulation of delamination in composite materials. NASA/TM-2002–211737 2002: 1–37. VA, USA.

[8] Turon A, Camanho PP, Costa J, Davila CG. An interface damage model for the simulation of delamination under variable-mode ratio in composite materials. NASA/TM-2004-213277 2004: VA, USA.

[9] Krueger R, Cvitkovich MK, O'Brien TK, Minguet PJ. Testing and analysis of composite skin/stringer debonding under multi-axial loading. Composite Material 2000; 34: 1263–1300.

[10] Zhao M, Gaedke R, Prinz. Mode II delamination behavior of carbon/epoxy composites. Advanced Composite Materials 2012; 4(2): 111-127.

[11] Camanho PP, Matthews FL. Delamination onset prediction in mechanically fastened joints in composite laminates. Composite Materials 1999; 33: 906-927.

[12] Campilho RG, Moura MF, Domingues JS. Using a cohesive damage model to predict the tensile behavior of CFRP single-strap repairs. Solids and Structures 2007; 45: 1497-1512.

[13] Davila CG, Camanho PP. Analysis of the effects of residual strains and defects on skin/stiffener debonding using decohesion elements. Proc. 44th AIAA/ASME/ ASCE/AHS Structures, Structural Dynamics, and Materials Conf, Norfolk, VA; April 7-10 2003.

[14] Koloor SSR, Tamin MN. Effects of lamina damage on flexural stiffness of CFRP composite laminates. 8th Asian-Australasian Conference on Composite Materials (ACCM-8), Kuala Lumpur, Malaysia; 6-8 November 2012.

[15] Abaqus 6.9-EF. Abaqus analysis user's manual 2011, Simulia.

[16] Sicot O, Rousseau J, Hearn D. Influence of stacking sequences on impact damage of pre-stressed isotropic composite laminates. 16th Int. Conf. on Composite Materials. Kyoto, Japan: July 2007.

[17] Yashiro S, Okabe T, Takeda N, Damage identification in a holed CFRP laminate using a chirped fiber Bragg grating sensor. Composites Science and Technology 2007; 67: 286–295.

[18] Arjmandi M. Damage evolution in carbon fiber-reinforced polymer (CFRP) composites under shear fatigue loading. M.Eng. Thesis 2012. Universiti Teknologi Malaysia.

[19] Davila CG, Camanho PP, Moura MF. Mixed-mode decohesion elements for analyses of progressive delamination. Proc. 42nd AIAA /ASME /ASCE /AHS /ASC Structures, Structural Dynamics and Materials Conf.; Seattle WA, USA 2001: 16–19.

[20] Benzeggagh ML, Kenane M. Measurement of mixed-mode delamination fracture toughness of unidirectional glass/epoxy composites with mixed-mode bending apparatus. Composites Science and Technology 1996; 49: 439-449.

[21] Reeder JR. An evaluation of mixed-mode delamination failure criteria. NASA/TM-104210 Feb 1992; VA, USA.